

From hard to soft diffraction and return

B.Z. Kopeliovich^a

^aMax-Planck-Institut für Kernphysik, Postfach 103980, 69029 Heidelberg, Germany
Joint Institute for Nuclear Research, Dubna, Russia

The long standing mystery of smallness of diffractive dissociation of hadrons to large effective masses (the Pomeron-proton cross section is only 2 mb) witnesses that the gluonic clouds of valence quarks are so small ($r_0 = 0.3\text{ fm}$) that soft interaction hardly resolves those gluons (diffraction is $\propto r_0^4$). A color-dipole light-cone (LC) approach is developed which incorporates a strong nonperturbative interaction of the LC gluons. The energy dependent part of the total hadronic cross section is calculated in a parameter-free way employing the nonperturbative LC wave functions of the quark-gluon Fock states. It rises with energy as s^Δ , and we predict $\Delta = 0.17 \pm 0.01$, as well as the normalization. However, the energy independent part of the cross section related to inelastic collisions with no gluon radiated (gluons are not resolved) cannot be calculated reliably and we treat it as an adjustable parameter which is fixed fitting just one experimental point for total cross section. Then the energy dependence of the total cross section (the Pomeron part) and the elastic slope are fully predicted, as well as the effective Pomeron trajectory in impact parameter space, in a good agreement with data. These results naturally explain the x -dependence of the diffractive DIS observed at HERA. Although diffraction is expected to be dominated by soft interactions the observed effective Δ is about twice as large as one (0.08) known for total cross sections. Diffractive excitations of large effective mass correspond to diffractive gluon radiation and should be associated with our calculated Δ .

1. Diffraction: evidence for small gluonic spots in the proton

The cross section of single diffraction in hadronic collisions (pp unless specified) can be expressed in terms of the so called Pomeron-proton total cross section [1,2],

$$\frac{d\sigma(pp \rightarrow pX)}{dt dM_X^2} \propto \sigma_{tot}^{Pp}. \quad (1)$$

What should one expect for σ_{tot}^{Pp} ? If to think about the Pomeron as a gluonic system its cross section contains the Cazimir factor $9/4$ compared to the meson-nucleon cross section. Thus, one may expect $\sigma_{tot}^{Pp} \sim 40 - 50\text{ mb}$. Such a naive estimate is, however, in a strict contradiction with data which show that the Pomeron interacts with a tiny cross section about 2 mb at high c.m. energy M_X [2]. This is the well know puzzling smallness of the triple-Pomeron coupling which was under intensive discussion back in 70s and is still waiting for a dynamical explanation.

Although the unitarity corrections suppress diffraction they cannot bridge such a large gap between the expectation and data. Indeed, nothing surprising comes out from the analysis [3] of the same data for the triple-Regge coupling \mathcal{IPPR} much larger than \mathcal{IPIP} . The corresponding Reggeon-proton cross section $\sigma_{tot}^{Rp} \approx 20\text{ mb}$ agrees with the expectation, and the absorptive corrections do not disturb it much.

The solution for the puzzling smallness of large-mass diffraction was suggested in [4]. Due to color screening (color transparency) the Pomeron-proton cross section depends quadratically on the size of the gluonic system. Indeed, glueballs are expected to be bound tighter than quarkonia [5], therefore to have smaller radii. Even the simple relation [6] between the color triplet (octet) string tension and the slope of Reggeon (Pomeron) trajectory, $\kappa = 1/(2\pi\alpha'_{R(P)})$, leads to the octet string tension which is at least four times larger than one for a triplet string (even more since the effective $\alpha'_{\mathcal{P}}$ is substantially increased by the unitarity corrections).

Thus, we should conclude that the strong non-perturbative interaction of gluons is responsible for smallness of large mass diffraction.

It worth reminding that the Pomeron is not a particle, but a shadow of inelastic processes, and the concept of Pomeron-proton cross section is ill defined (except if the Pomeron is a true Regge pole). We use this concept here in order to impose a scale which shows that the diffractive cross section is abnormally small. In what follows we employ the light-cone (LC) QCD formalism which relates the observed suppression of diffraction to the smallness of gluonic spots inside the proton. Indeed, the observed dependence of the cross section Eq. (1), $1/M_X^2$, can only be due to diffractive radiation of gluons since they are vector particles. The interaction with the target should be sufficiently hard to resolve the gluonic fluctuation in a valence quark. The smaller is the gluon cloud of a valence quark, the more difficult is to excite it. If the LC wave function of the proton is dominated by configurations in which gluons are located around the valence quarks at small transverse distances $\sim r_0$, then the amplitude of diffraction is proportional to r_0^2 and the cross section of diffractive gluon radiation is suppressed as r_0^4 . Therefore, high-mass diffraction is a very sensitive tool to study the gluonic structure of the proton. The related formalism based on the LC Green function approach is presented below.

2. From hard to soft diffraction

The first correct pQCD calculation for large-mass diffraction cross section in DIS was performed in [7] in the LC dipole representation. The diffractive cross section of gluon radiation $qN \rightarrow qGN$ is given by Eqs. (64) of [4] (see simple derivation in Appendix A.2 of [4]),

$$\begin{aligned} & \frac{M^2 d\sigma(qN \rightarrow qGN)}{dM^2 dq_T^2} \Big|_{q_T=0} \\ &= \frac{81}{1024\pi} \int d^2\rho \left| \Psi_{qG}(\alpha, \vec{\rho}) \sigma_{\bar{q}q}(\rho, \bar{s}) \right|^2_{\alpha \ll 1}, \quad (2) \end{aligned}$$

where q_T is the transverse momentum of the radiated gluon, M is the quark-gluon effective mass, α is the fraction of the initial LC momentum of

the quark taken away by the gluon; $\sigma_{\bar{q}q}(\rho, s)$ is the cross section of interaction with a nucleon of a $\bar{q}q$ dipole with separation ρ and energy s . The perturbative quark-gluon (photon) LC wave function is derived in [8] (see also in [9]). Using it one ends up with diffraction which grossly overestimates data for $pp \rightarrow pX$, as one might has expected in view of discussion in previous section.

Of course one should not apply pQCD methods to the soft reaction, at small q_T the final quark and gluon cannot be treated as free particles since they should experience a strong nonperturbative interaction comoving with a large transverse separation along the light cone. Propagation of such a qG pair from initial longitudinal coordinate z_1 and separation $\vec{\rho}_1$ to final z_2 , $\vec{\rho}_2$ is described by the Schrödinger equation [4],

$$\begin{aligned} i \frac{d}{dz_2} G_{qG}(z_1, \vec{\rho}_1; z_2, \vec{\rho}_2) = & \left[\frac{m_q^2 - \Delta_\rho}{2p\alpha(1-\alpha)} \right. \\ & \left. + V_{\bar{q}q}(z_2, \vec{\rho}, \alpha) \right] G_{qG}(z_1, \vec{\rho}_1; z_2, \vec{\rho}_2). \quad (3) \end{aligned}$$

The first term in square brackets is the kinetic one, the LC potential is real for propagation in vacuum and describes the quark-gluon interaction. We choose it in the oscillator form in order to solve (3) analytically,

$$\text{Re } V_{qG}(z_2, \vec{\rho}, \alpha) = \frac{b^4(\alpha) \vec{\rho}^2}{2p\alpha(1-\alpha)}, \quad (4)$$

where $b^2(\alpha) = b_0^2 + 4b_1^2\alpha(1-\alpha)$. Since we are interested in $\alpha \ll 1$, $b(\alpha) = b_0$.

As far as the Green function is known one can calculate the nonperturbative LC wave function for a quark-gluon Fock state,

$$\begin{aligned} \Psi_{qG}(\vec{\rho}, \alpha) = & \frac{i\sqrt{\alpha_s/3}}{2\pi p\alpha(1-\alpha)} \\ & \times \int_{-\infty}^{z_2} dz_1 (\bar{\chi} \hat{\Gamma} \chi) G_{qG}(z_1, \vec{\rho}_1; z_2, \vec{\rho}) \Big|_{\rho_1=0} \quad (5) \end{aligned}$$

where χ , $\bar{\chi}$ are the initial or final quark spinors, and the vertex function reads,

$$\begin{aligned} \hat{\Gamma} = & im_q \alpha^2 \vec{e}^* \cdot (\vec{n} \times \vec{\sigma}) + \alpha \vec{e}^* \cdot (\vec{\sigma} \times \vec{\nabla}) \\ & - i(2-\alpha) \vec{e}^* \cdot \vec{\nabla}, \quad (6) \end{aligned}$$

which has a rather simple form,

$$\Psi_{qG}(\vec{r}, \alpha \ll 1) = -\frac{2i}{\pi} \sqrt{\frac{\alpha_s}{3}} \frac{\vec{e}^* \cdot \vec{r}}{r^2} e^{-r^2 b_0^2/2}, \quad (7)$$

where \vec{e} is the polarization vector of the gluon. This wave function recovers the perturbative one [9] in the limit of $b_0 \rightarrow 0$.

Comparing the cross section of diffractive gluon radiation with data one arrives at a rather large value of $b_0 = 0.65 \text{ GeV}$ corresponding to a short mean quark-gluon separation $r_0 = 1/b_0 = 0.3 \text{ fm}$. This is one of the central results of [4].

3. Small gluonic spots and the total pp cross section

Using the same approach one can calculate the cross section of gluon bremsstrahlung (nondiffractive) by a $\bar{q}q$ meson [4,10,11],

$$\begin{aligned} \sigma_1^{hN} &= \int_0^1 d\alpha_q \int d^2 R \left| \Psi_{\bar{q}q}^h(R, \alpha_q) \right|^2 \\ &\times \frac{9}{4} \int_{\alpha \ll 1} \frac{d\alpha}{\alpha} \int d^2 r \left\{ \left| \Psi_{\bar{q}G}(\vec{R} + \vec{r}, \alpha) \right|^2 \right. \\ &\times \sigma_{\bar{q}q}^N(\vec{R} + \vec{r}) + \left| \Psi_{qG}(\vec{r}, \alpha) \right|^2 \sigma_{\bar{q}q}^N(r) \\ &- \text{Re } \Psi_{qG}^*(\vec{r}, \alpha) \Psi_{\bar{q}G}(\vec{R} + \vec{r}, \alpha) \\ &\times \left. \left[\sigma_{\bar{q}q}^N(\vec{R} + \vec{r}) + \sigma_{\bar{q}q}^N(r) - \sigma_{\bar{q}q}^N(R) \right] \right\}, \end{aligned} \quad (8)$$

where \vec{R} and \vec{r} are the $\bar{q}q$ and Gq transverse separations respectively. Making use of relation $\langle r^2 \rangle \ll \langle R^2 \rangle$ one can keep only the second term in the curly brackets what makes further calculations rather simple.

The cross section of gluon bremsstrahlung by a quark interacting with a nucleon is found [10,11] to be,

$$\sigma_{rad}^{qN} = \sum_{n=1} \frac{1}{n!} \left[\frac{4 \alpha_s}{3 \pi} \ln \left(\frac{s}{s_0} \right) \right]^n \frac{9}{4} C r_0^2. \quad (9)$$

Since the mean separation r_0 is small, one can use the approximation $\sigma_{\bar{q}q}(r) \approx C r^2$, where $C \approx 2.3$ can be evaluated perturbatively. The QCD coupling α_s was averaged over the radiation spectrum with a result $\alpha_s = 0.38 - 0.43$ in a good

agreement with the critical value $\alpha_c = 0.43$ evaluated in [12].

To obtain the total pp cross section one should add the cross section of pp interaction without any gluon radiation. This contribution, σ_0^{pp} is pure nonperturbative and cannot be evaluated reliably. We treat it as a free parameter. Thus, the total pp cross section takes the form,

$$\sigma_{tot}^{pp} = \tilde{\sigma}_0^{pp} + \frac{27}{4} C r_0^2 \left(\frac{s}{s_0} \right)^\Delta, \quad (10)$$

with

$$\Delta = \frac{4 \alpha_s}{3 \pi} = 0.17 \pm 0.01, \quad (11)$$

and $\tilde{\sigma}_0^{pp} = \sigma_0^{pp} - 9Cr_0^2/4$.

This value of Δ is about twice as large as the one suggested by the data for the energy dependence of total pp cross sections when the simple parameterization $\sigma_{tot}^{pp} \propto s^\Delta$ is applied. However, the radiative part is a rather small fraction of the total cross section (at medium high energies) and the presence of the energy independent term σ_0 substantially reduces the effective Δ_{eff} .

4. Unitarization and comparison with data

The cross section (10) apparently violates the Froissart bound and one should introduce unitarity corrections [13]. Unfortunately, this is not a well defined procedure since different recipes can be found in the literature.

The simplest known way to restore unitarity is to eikonalize the partial amplitude $\gamma_{IP}(b, s)$,

$$\text{Im } \Gamma_{IP}(b, s) = 1 - \exp \left[-\text{Im } \gamma_{IP}(b, s) \right]. \quad (12)$$

At very high s this amplitude approaches the black disk limit [13], $\text{Im } \Gamma_{IP}(s, b) \rightarrow \Theta[R^2(s) - b^2]$, with radius, $R(s) = r_0 \Delta \ln(s/s_0)$. Correspondingly, at asymptotic energies,

$$\Delta \ln \left(\frac{s}{s_0} \right) \gg \frac{\langle r_{ch}^2 \rangle}{r_0^2}, \quad (13)$$

all hadronic cross sections reach the maximal universal energy growth allowed by Froissart-Martin's bound,

$$\sigma_{tot}^{hN}(s) \rightarrow 2 \pi r_0^2 \Delta^2 \ln^2 \left(\frac{s}{s_0} \right). \quad (14)$$

The eikonalization procedure (12) would be suitable if the the incoming hadrons were eigenstates of the interaction [14]. Hadrons, however, are subject to diffractive off-diagonal excitation, and the eikonal form of unitarization should be corrected in a way similar to Gribov's inelastic corrections for hadron–nucleus cross sections. The lowest order unitarity correction in (12) comes from the quadratic term in the exponent expansion of $\Gamma(b, s)$. It has to be modified using the AGK cutting rules to include single diffraction,

$$\begin{aligned} \text{Im } \Gamma_{\mathcal{P}} &= \text{Im } \gamma_{\mathcal{P}} - \frac{1}{2} \left(\text{Im } \gamma_{\mathcal{P}} \right)^2 \left[1 + D(s) \right] \\ &+ O(\gamma_{\mathcal{P}}^3), \end{aligned} \quad (15)$$

where $D(s) = \sigma_{sd}(s)/\sigma_{el}(s)$ is approximately 0.25 in the ISR energy range and decreases slightly with energy $\propto s^{-0.04}$ [15] due to stronger unitarity corrections. Asymptotically, as $s \rightarrow \infty$, $D(s)$ vanishes since $\sigma_{el}(s) \propto \ln^2 s$ and $\sigma_{sd}(s) \propto \ln s$.

The inelastic corrections to higher order terms in the expansion (12) are poorly known. A simple way to keep (15) and to include diffraction into the higher terms is to modify (12) as,

$$\begin{aligned} \text{Im } \Gamma_{\mathcal{P}}(b, s) &= \frac{1}{1 + D(s)} \\ &\times \left\{ 1 - \exp \left[- \left(1 + D(s) \right) \text{Im } \gamma_{\mathcal{P}}(b, s) \right] \right\} \end{aligned} \quad (16)$$

which is known as quasi-eikonal model [2].

Following [16] we assume that the t -dependence of the pp elastic amplitude is given by the Dirac electromagnetic formfactor squared. Correspondingly, the mean square radius $\langle \tilde{r}_{ch}^2 \rangle$ evaluated in [16] is smaller than $\langle r_{ch}^2 \rangle$.

For the dipole parameterization of the formfactor the partial elastic amplitude which is related via unitarity to the n th term in the radiation cross section (9) takes the form,

$$\text{Im } \gamma_n^{pp}(b, s) = \frac{\sigma_n^{pp}(s)}{8 \pi B_n} y^3 K_3(y), \quad (17)$$

where $K_3(y)$ is the third order modified Bessel function and $y = b\sqrt{8/B_n}$. The slope parameter grows linearly with n due to random walk of radiated gluons with a step r_0^2 in the impact parameter plane, $B_n = 2\langle \tilde{r}_{ch}^2 \rangle / 3 + n r_0^2$.

In order to calculate the total cross section, $\sigma_{tot} = 2 \int d^2 b \text{Im} \Gamma(b, s)$, one needs to fix the energy independent term with $n = 0$ in (10). This can be done comparing with the data for σ_{tot} at any energy sufficiently high to neglect Reggeons. We use the most precise data [17] at $\sqrt{s} = 546 \text{ GeV}$ and fix $\tilde{\sigma}_0 = 39.7 \text{ mb}$.

The predicted energy dependence of σ_{tot}^{pp} shown by the dashed curve in Fig. 1 is in good agreement

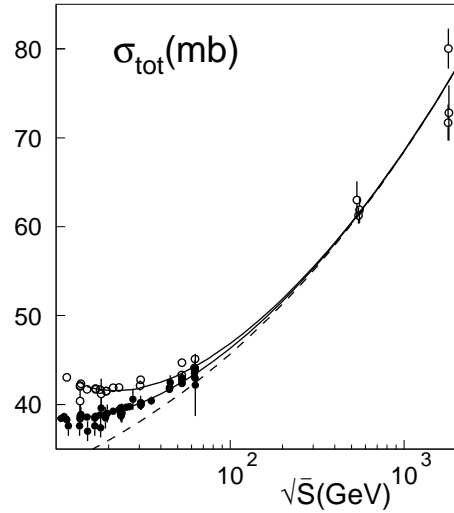


Figure 1. Data for total pp (full circles) and $\bar{p}p$ (open circles) cross section and the prediction of Eq. (17) for the energy dependence of the Pomeron part (dashed curve) and including Reggeon contribution (solid curves).

with the data at high energies, but apparently needs Reggeon corrections towards low energies.

In order to improve description of data at medium high energies (ISR) we added the contribution of leading Reggeons parameterized in the standard way with common parameters for pp and $\bar{p}p$, the intercept fixed at $\alpha_R(0) = 1/2$ and the slope parameter $\alpha'_R = 0.9 \text{ GeV}^{-2}$. The Reggeons are added directly in the partial elastic amplitude,

$$\begin{aligned} \text{Im } \Gamma(s, b) &= \text{Im } \Gamma_{\mathcal{P}}(s, b) \\ &+ \Gamma_R(s, b) \left[1 - \text{Im } \Gamma_{\mathcal{P}}(s, b) \right], \end{aligned} \quad (18)$$

with a proper screening by absorptive corrections. The results are shown by the solid curves of Fig. 1 (pp bottom curve and $\bar{p}p$ upper curve).

Employing Eq. (16) we can also predict the slope of elastic scattering at $t = 0$, $B_{el}(s) = \langle b^2 \rangle / 2$, where averaging is weighted by the partial amplitude (16). The results exhibit good agreement when compared with the pp and $\bar{p}p$ data in Fig. 2.

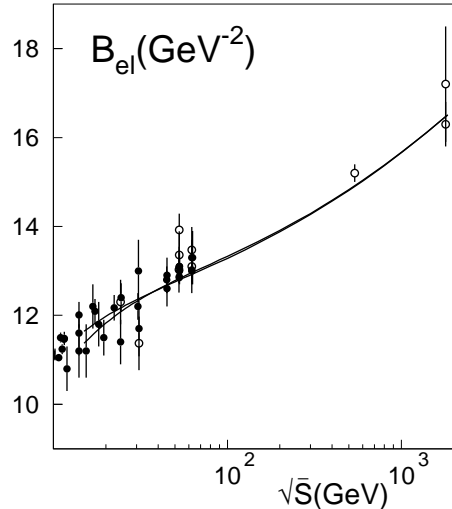


Figure 2. Data for the elastic slope and our predictions. The upper and bottom curves and open and full circles correspond to $\bar{p}p$ and pp respectively.

Note that the the slope essentially depends on our choice of $\langle \tilde{r}_{ch}^2 \rangle$ in (17), however the predicted energy dependence, *i.e.* the effective value $\alpha'_{\mathcal{P}}$ is fully defined by the parameter r_0 fixed in [4]. Indeed, each radiated gluon makes a small “step” $\sim r_0^2 = 0.1 \text{ fm}^2$ in the impact parameter plane leading to the rising energy dependence of the elastic slope. Eventually, at very high energies the approximation of small gluon clouds should break down. Nevertheless, the mean number of gluons in a quark $\langle n \rangle = \Delta \ln(s/s_0)$ remains quite small in the energy range of colliders. It is only $\langle n \rangle = 0.7 - 1$ at the ISR and reaches about two gluons at the Tevatron. Correspondingly, the mean square of

the quark radius grows from 0.06 fm^2 to 0.18 fm^2 which is still rather small compared to the mean square of the charge radius of the proton.

5. Pomeron trajectory in impact parameter space

Actually, we know more about the elastic partial amplitude than just integral characteristics like the total cross section and slope, we know the shape of b -dependence. To compare the b -distribution and its development with energy directly with experimental data an analysis similar to one which has been done by Amaldi and Schubert [18] was performed recently in [11]. The data for differential elastic cross section was fitted, including both the real and imaginary parts of the amplitude, and then Fourier transformed to impact parameter representation. As different from [18], no model dependence was involved (geometrical scaling was assumed in [18]) and data from the S $\bar{p}p$ S at $\sqrt{s} = 540 \text{ GeV}$ were included in addition to data from the ISR. The data for partial elastic amplitude as function of impact parameter are plotted in Fig. 3 in comparison with our predictions based on Eq. (18). Agreement between the data and our predictions is remarkably good, especially if to recall that the Pomeron part has no free parameters, except one, $\tilde{\sigma}_0$, adjusted to the total cross section measured at one energy $\sqrt{s} = 546 \text{ GeV}$ [17]. Both the predicted shape of the partial amplitude and its energy development are confirmed by the data.

Addition of the $S\bar{p}pS$ data at $\sqrt{s} = 540 \text{ GeV}$ into the analysis plays a crucial role, it substantially increases the energy range important for study of energy dependent effects. In particular it helps to extract from the data the effective Pomeron trajectory $\alpha_{\mathcal{P}}(b) = 1 + \Delta(b)$ as function of impact parameter, describing energy dependence $s^{\Delta(b)}$ of the partial elastic amplitude. The results are depicted in Fig. 4. The solid curves show the slope of energy dependence calculated with Eq. (18) without any adjustment. The agreement is rather good.

The simple parameterization of the amplitude by a single Pomeron pole without unitarity corrections fitted to data for total cross section and

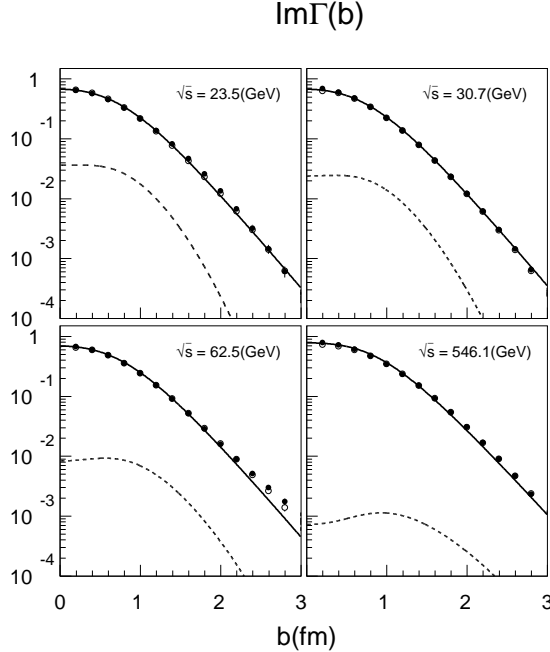


Figure 3. The imaginary part of the partial amplitude $\text{Im}\Gamma(b)$ as function of impact parameter at different c.m. energies. The solid curves are the theoretical prediction with Eq. (18), and the dashed curves show the contribution of Reggeons.

elastic slope [19] corresponds to the dashed curve. Although this parameterization is very successful describing total cross section it poorly reproduces energy dependence of the partial amplitude at different impact parameters. At the same time we should notice that the wide spread prejudice that this model leads to a precocious breaking of unitarity at small b is incorrect. We see from Fig. 4 that $\Delta(b=0)$ predicted by this simple model is rather small. In the case of geometrical scaling it would be zero.

6. Back to hard diffraction: Do we understand the results from HERA?

Diffraction of highly virtual photons, $\gamma^* p \rightarrow X p$ observed at HERA is expected to be dominated by soft processes [20]. Indeed, the dominant *hard* fluctuations of the photon, have a small

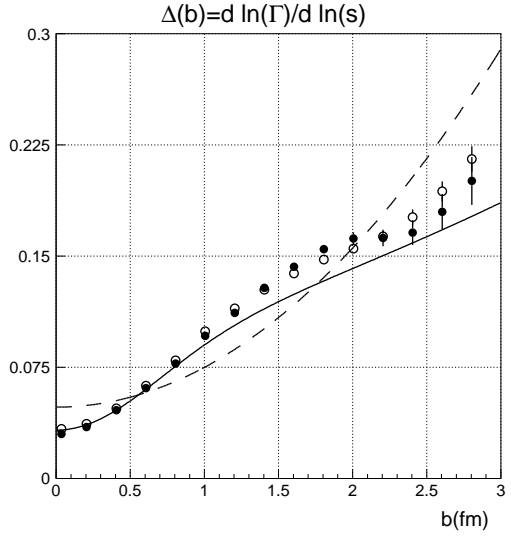


Figure 4. The effective Pomeron trajectory in impact parameter space. Black and open points correspond to different parameterization of the t -dependent elastic amplitude. Our prediction and of the single Pomeron pole model are shown by solid and dashed curves respectively.

transverse size $\sim 1/Q^2$, therefore the diffraction cross section is tiny, $\sim 1/Q^4$. On the other hand, *soft* fluctuations of large size which appear very rarely with probability $\sim 1/Q^2$ (for transverse photons), interact with a large hadronic cross section, therefore they dominate the “hard” DIS diffraction. Consequently, one might expect that the cross section should rise with energy (at fixed Q^2) like the hadronic cross sections, $\propto s^{0.08}$. However, a much steeper slope of energy dependence was observed at HERA. According to the analysis in [21] data from the H1 and ZEUS experiments lead to

$$\begin{aligned} \Delta &= 0.2 \pm 0.02 \quad (\text{H1}), \\ \Delta &= 0.13 \pm 0.04 \quad (\text{ZEUS}). \end{aligned} \quad (19)$$

The source of excitations with large effective masses is diffractive gluon bremsstrahlung related via unitarity to the energy dependent second term in the elastic amplitude (total cross section) in

Eq. (10). At the same time, small mass diffraction is governed by excitation of the $\bar{q}q$ fluctuation in the photon without gluon radiation (yet it may include radiation of energetic gluons). This diffractive component is related by unitarity to the first energy independent term in Eq. (10). Therefore, for large excitation masses we should expect about the same value of Δ given by Eq. (11), rather than the averaged effective value ~ 0.08 fitted to the total cross section.

Formulating differently, we can say that the softest part of interaction responsible for the constant term in the total cross section Eq. (10) is related to the large size R of the valence quark skeleton. Such interaction is too soft to resolve the gluon clouds of small size r_0 . It needs a semi-hard interaction with transverse momentum $\sim 1 \text{ GeV}$ to shake off the gluons from the quarks. This part of interaction is responsible for the energy dependent term in (10) and for diffractive gluon radiation, *i.e.* excitation of large effective mass.

7. Summary

Our main observation is existence of small gluonic clouds surrounding the valence quarks in light hadrons. The most soft part of interaction with transverse wave length longer than these spots cannot either resolve them or shake them off the quarks. As an example, it can be treated in the string model as a crossing and rearrangement of the hadronic strings. The corresponding part of the total cross section is energy independent since the size of the valence quark skeleton does not grow with energy.

On the contrary, the gluon spots do rise with energy since the gluon population increases and they perform a Braunian motion in the transverse plane. The gluon bremsstrahlung cross section also rises since each gluon can be radiated at different rapidities with about the same probability. This is the source of energy dependence of the total cross section.

Such a two-scale picture of interaction leads to presence of the two terms in the total cross section Eq. (10). The first one is energy independent, and the second one rises as power of energy with quite

a large exponent given by (11). This second term is fully predicted, not only its energy dependence, but also the normalization. Only the first energy-independent term is treated as a free parameter and is fixed by fitting just one experimental point.

Our calculations reproduce well the energy dependence of the total pp cross section, and the elastic slope. Moreover, the data for differential elastic scattering Fourier transformed to impact parameter representation also well agree with our predictions, including the effective Pomeron trajectory in impact parameter space.

The two components of the total cross section can be well separated in diffractive dissociation. Indeed, the small mass diffraction corresponds to excitation of the quark ensemble without gluon radiation, *i.e.* it is energy independent. Only diffractive excitation of gluon clouds leads to the large mass dissociation, called in Regge phenomenology triple-Pomeron diffraction. This part is rather small, but steeply rises with energy with the power given by (10). This indeed has been observed by experiments at HERA.

We have found a new regime where one can perform calculations employing the smallness of the size $r_0 = 0.3 \text{ fm}$ of the gluonic spots compared to large interquark separation $R \sim 1 \text{ fm}$. On the contrary, in DIS one deals with an opposite limit when the gluon clouds are much larger than the interquark separation. In that case the cross section can be estimated using perturbative QCD provided that $Q^2 \gg Q_0^2$ ($Q_0 \sim 1 \text{ GeV}$), and $s \gg s_0$ ($s_0 \sim 1 \text{ GeV}^2$), but $x = Q^2/s \ll 1$. Dependent on the approximation used, two models for the Pomeron are known, the BFKL [22] and double-leading-log approximation. The total virtual photoabsorption cross section is predicted to rise steeply with energy as is confirmed by data from HERA.

Our conclusion about smallness of gluonic spots in light hadrons is in a good accord with what has been already observed in models for nonperturbative QCD vacuum. It has been found employing the QCD sum rules [23] that the gluonic formfactor of the proton has very weak Q^2 dependence corresponding to a small radius of the gluon distribution $\sim 0.3 \text{ fm}$. A small gluon correlation radius $\sim 0.3 \text{ fm}$ also appears in the lattice

calculations [24]. It is also predicted by the model of instanton liquid [25]. Experimental observation of a small cross section for large mass soft diffractive dissociation which has led the analyses [4] to a small value of r_0 can be treated more generally, in particular as a confirmation for a small size cloud of any kind of gluonic vacuum fluctuations surrounding the valence quarks. They are usually referred to as constituent quarks.

Note that the two-scale structure of the energy-dependent total cross section has to exist also in other models attempting to incorporate the non-perturbative effects [26,27].

Acknowledgment: I am grateful to the Organizing Committee for kind invitation and financial support.

REFERENCES

1. A. Mueller, Phys. Rev. **D2** (1970) 2963; **D4** (1971) 150
2. A.B. Kaidalov, Phys. Rept. **50** (1979) 157
3. Yu.M. Kazarinov, B.Z. Kopeliovich, L.I. Lapidus and I.K. Potashnikova, JETP **70**, 1152 (1976).
4. B.Z. Kopeliovich, A. Schäfer and A.V. Tarasov, Phys. Rev. **D62** (2000) 054022.
5. V. Novikov, M. Shifman, A. Veinshtein and V. Zakharov, Nucl. Phys. **B191** 301
6. A. Casher, H. Neubereger and S. Nussinov, Phys. Rev. **D20** (1979) 179.
7. J. Bartels, H. Jung and M. Wüsthoff, Quark-Antiquark-Gluon Jets in DIS diffractive dissociation, hep-ph/9903265
8. B.Z. Kopeliovich, Soft Component of Hard Reactions and Nuclear Shadowing (DIS, Drell-Yan reaction, heavy quark production), in proc. of the Workshop Hirschegg'95: Dynamical Properties of Hadrons in Nuclear Matter, Hirschegg, January 16-21,1995, ed. by H. Feldmeier and W. Nörenberg, Darmstadt, 1995, p. 102 (hep-ph/9609385)
9. B.Z. Kopeliovich, A. Schäfer and A.V. Tarasov, Phys. Rev. **C59** (1999) 1609 (extended version in hep-ph/9808378)
10. B.Z. Kopeliovich, I.K. Potashnikova, B. Povh and E. Predazzi, Phys. Rev. Lett. **85** (2000) 507
11. B.Z. Kopeliovich, I.K. Potashnikova, B. Povh and E. Predazzi, *Soft QCD Dynamics of Elastic Scattering in Impact Parameter Representation*, hep-ph/0009008, to appear in Phys. Rev. **D**
12. V.N. Gribov, Eur. Phys. J. **C10** (1999) 71; *ibid* **C10**, 91 (1999).
13. M.I. Dubovikov, B.Z. Kopeliovich, L.I. Lapidus and K.A. Ter-Martirosyan, Nucl. Phys. **B123** (1977) 147.
14. Al.B. Zamolodchikov, B.Z. Kopeliovich and L.I. Lapidus, Sov. Phys. JETP Lett. **33** (1981) 612.
15. K. Goulianos, J. Montanha, Phys. Rev. **D59** (1999) 114017.
16. J. Hüfner and B. Povh, Phys. Rev. **D46** (1992) 990.
17. F. Abe et al., Phys. Rev. **D50**, 550 (1993).
18. U. Amaldi and K.R. Schubert, Nucl. Phys. **B166** (1980) 301.
19. Review of Particle Properties, Phys. Rev. **D54** (1996) 1.
20. B.Z. Kopeliovich and B. Povh, Phys. Lett. B367 (1996) 329; Z. Phys. **A356** (1997) 467.
21. C. Royon et al., *QCD analysis of the diffractive structure function $F_2^{D(3)}$* , hep-ph/0010015
22. E.A. Kuraev, L.N. Lipatov and V.S. Fadin, Sov. Phys. JETP **44** (1976) 443 ; **45** (1977) 199; Ya.Ya. Balitskii and L.I. Lipatov, Sov. J. Nucl. Phys. **28** (1978) 822; L.N. Lipatov, Sov. Phys. JETP **63** (1986) 904.
23. V.M. Braun, P. Górnicki, I. Mankiewicz and A. Schäfer, Phys. Lett. **B302** (1993) 291.
24. M. D'Elia, A. Di Giacomo and E. Meggiolaro, Phys. Lett. **B408**, 315 (1997).
25. T. Schäfer, E.V. Shuryak, Rev. Mod. Phys. **70**, 323 (1998).
26. D. Kharzeev and E.M. Levin, Nucl.Phys. **B578** (2000) 351.
27. D. Kharzeev, Yu. Kovchegov and E.M. Levin, *QCD Instantons and the Soft Pomeron*, hep-ph/0007182.